Time Dependent Growth of the Block Copolymer P123 Micelles near Cloud Point: Employing Heat Cycling as a Tool to form Kinetically Stable Wormlike Micelles

ARTICLE *in* THE JOURNAL OF PHYSICAL CHEMISTRY B · AUGUST 2009

Impact Factor: 3.3 · DOI: 10.1021/jp900535f · Source: PubMed

3 AUTHORS:

Rajib Ganguly
Bhabha Atomic Research Centre
61 PUBLICATIONS **918** CITATIONS
SEE PROFILE

Manoj Kumbhakar
Government of India
65 PUBLICATIONS **1,548** CITATIONS
SEE PROFILE

Vinod K Aswal
Bhabha Atomic Research Centre
392 PUBLICATIONS **4,905** CITATIONS
SEE PROFILE

Time Dependent Growth of the Block Copolymer P123 Micelles near Cloud Point: Employing Heat Cycling as a Tool to form Kinetically Stable Wormlike Micelles

R. Ganguly,*,† M. Kumbhakar,‡ and V. K. Aswal§

Chemistry Division, Radiation & Photochemistry Division, and Solid State Physics Division, Bhabha Atomic Research Center, Mumbai 400 085, India

Received: January 19, 2009; Revised Manuscript Received: May 27, 2009

The sphere-to-rod growth behavior of the triblock copolymer $EO_{20}PO_{70}EO_{20}$ (P123) micelles has been studied in an aqueous medium by dynamic light scattering (DLS), viscometry, and small angle neutron scattering (SANS) techniques. Unlike the other aqueous pluronic systems, the P123 solutions show a time dependent sphere-to-rod micellar growth in the aqueous medium on approaching their cloud points. The rate of micellar growth increases with increase in temperature, but quite interestingly, it improves rather dramatically when the copolymer solutions are subjected to heat cycling, i.e., heating them to the phase separation and subsequently cooling them back to below their cloud points. The observed kinetically restricted micellar growth has been attributed to the slow dynamics of the micellar restructuring processes essential to arrive at the temperature dependent equilibrium structure. It has been suggested that the improvement in the micellar growth rate upon heat cycling is due to overcoming of the activation energy associated with the micellar restructuring process. In the presence of water-structure-making salts like NaCl, such heat cycling produces kinetically stable wormlike micelles at room temperature, which is observed for the first time in the aqueous pluronic systems.

Introduction

The polyethylene oxide−polypropylene oxide−polyethylene oxide (PEO−PPO−PEO) based triblock copolymers have been subjected to extensive investigations because of their rich structural polymorphism and numerous industrial applications.[1−13] The uniqueness of these copolymers vis-à-vis the conventional nonionic surfactants is that they show a strong temperature dependence in their self-assembly characteristics in the aqueous medium.[10] At low temperature, both the PPO and PEO blocks are soluble in water and the copolymer molecules remain in the form of unimers. As the PPO blocks become insoluble at the critical micellar temperature (CMT), these molecules start forming spherical micelles, which remain in equilibrium with the unimers.[11−13] The micelles formed undergo restructuring with an increase in temperature, leading to an increase in their aggregation number and core size, and a decrease in their degree of hydration.[11,14,15] For some of the copolymers, such restructuring processes lead to a sphere-to-rod micellar shape change when the size of the core becomes equal to the length of the stretched PPO chain.[16] At still higher temperature, large micellar clusters start forming, the concentration of which increases with an increase in temperature until the copolymer solution phase separates at the cloud point (CP).[17−19]

A study on the dynamics of the aggregation of the block copolymer in the aqueous medium identifies three types of relaxation processes operative between the CMT and the CP of the copolymer solutions. These are associated with the incorporation of the copolymer unimers into the micelles, the restructuring of the micelles with increase in temperature, and the formation of micellar clusters near the CP.[19,20] The second relaxation process has been found to slow down significantly with an increase in the molecular weight of the copolymer molecules and also has an activation barrier associated with it.[19] Although the aggregation processes of these copolymers have been studied in great detail as a function of temperature and the copolymer concentration, the studies on the time dependence in the micellar growth and restructuring process as direct fallout of the presence of an activation barrier in the micellar restructuring process has never been explored. In view of this, we have carried out a systematic study on the growth behavior of the $EO_{20}PO_{70}EO_{20}$ (Pluronic P123) micelles as a function of time on approaching the cloud point of the copolymer solutions. P123 is chosen in view of its higher molecular weight than the pluronics P85 (MW $\approx$ 4600), P84 (MW $\approx$ 4200), and L64 (MW $\approx$ 2900), which show sphere-to-rod micellar shape transition in the aqueous medium. Since the observed micellar shape transition in the aqueous solutions of these three copolymers has been quite fast considering the time scale of their size and viscosity measurement, no time dependence of their growth behavior has been reported. The copolymers with an even larger molecular weight like F127 (MW $\approx$ 12600), F68 (MW $\approx$ 8400), F88 (MW $\approx$ 11400), etc., on the other hand, do not show similar shape transition of their micelles because of their highly hydrophilic nature. The studies carried out by us show a time dependent sphere-to-rod micellar growth in the aqueous P123 solutions on approaching their cloud points, the rate of which undergoes remarkable improvement when the copolymer solutions are subjected to thermal heat cycling.

Experimental Section

Materials and Sample Preparation. The triblock copolymer $EO_{20}PO_{70}EO_{20}$ (Pluronic P123) was procured from Aldrich. Sodium chloride was purchased from Merck, and pyrene was obtained from Baker Chemical Co., New Jersey. The copolymer solutions were prepared by weighing required amounts of water,

* Corresponding author. E-mail: rajibg@barc.gov.in, rajugang@yahoo.co.in. Phone: +91-22-25590286. Fax: +91-22-25505150.
† Chemistry Division.
‡ Radiation & Photochemistry Division.
§ Solid State Physics Division.

10.1021/jp900535f CCC: $40.75
Published on Web 06/18/2009

copolymer, and salt (when needed) and keeping them in a refrigerator in tightly closed glass stoppered vials for about 1 week.

Methods

Viscometry. The absolute viscosities of the solutions at different temperatures were measured by using calibrated Cannon Ubbelohde viscometers[21] in a temperature controlled water bath.

Dynamic Light Scattering (DLS). DLS measurements of the solutions were performed using a Malvern 4800 Autosizer employing a 7132 digital correlator. The light source was argon ion laser operated at 514.5 nm with a maximum output power of 2 W. The average decay rate was obtained by analyzing the electric field autocorrelation function $g^1(\tau)$ vs time data using a modified cumulants method or a stretched biexponential equation.[22−25] The modified cumulants method overcomes the limitations of cumulants analysis to fit the data at long correlation time in the presence of large polydispersity. In the case of aqueous pluronic solutions, the DLS data of the rodlike micelles show large polydispersity primarily because of the presence of a small amount of spherical micelles along with the rodlike micelles. The cumulants method, which is good for analyzing the correlation function data with low polydispersity, shows a large deviation from the correlation function data of these systems at large correlation time. The modified cumulant method overcomes this limitation and thus was found to be suitable for this system.[26] For generating the average decay rate (Γ) vs q^2 plots (q being the magnitude of the scattering vector given by $q = [4\pi n \sin(\theta/2)]/\lambda$, where n is the refractive index of the solvent, λ is the wavelength of laser light, and θ is the scattering angle. Measurements were made at five different angles ranging from 50 to 130°. The change in the refractive index and the viscosity of water upon addition of salt were taken into account while analyzing the correlation function data. The apparent equivalent hydrodynamic radii of the micelles were calculated using the Stokes−Einstein relationship. For anisotropic micelles, the lengths of the micelles were estimated from the translational diffusion coefficient employing Perrin's formula. For prolate ellipsoids, the diffusion coefficient (D) is related to the axial ratio (ρ) and semimajor axis (a) of the micelles, by the relation[27]

$$D = kT[G(\rho)]/6\pi\eta a$$

$$G(\rho) = (1 - \rho^2)^{-1/2} \ln[\{1 + (1 - \rho^2)^{1/2}\}/\rho] \qquad (1)$$

where D is the translational diffusion coefficient, ρ is the ratio of the semiminor axis to the semimajor axis with a value of <1, and η is the viscosity of the medium. The semiminor axis is fixed as the radius of the spherical micelle before the onset of growth.

Small Angle Neutron Scattering (SANS). SANS measurements were carried out on the samples prepared in D_2O at the SANS facility at DHRUVA reactor, Trombay. The mean incident wavelength was 5.2 Å with $\Delta\lambda/\lambda = 15\%$. The scattering was measured in the scattering vector (q) range of 0.017−0.3 $Å^{-1}$. The measured SANS data were corrected for the background, the empty cell contributions, and the transmission, and were placed on an absolute scale using standard protocols. Correction due to the instrumental smearing was taken into account throughout the data analysis.[28]

The differential scattering cross section per unit volume ($d\Sigma/d\Omega$) of monodisperse micelles can be written as[29,30]

$$d\Sigma/d\Omega = NF_{mic}(q)S(q) + B \qquad (2)$$

N is the number density of the micelles, and B is a constant term that represents the incoherent background scattering mainly from the hydrogen atoms present in the sample. $F_{mic}(q)$ is the form factor characteristic of a specific size and shape of the scatterers, and $S(q)$ is the structure factor that accounts for the interparticle interaction. The block copolymer micelles can be considered as a core−shell particle with different scattering length densities of the core and the shell. The structure of these micelles is described using a model consisting of PEO chains attached to the surface of the PPO core.[29,30] The form factors for spherical and ellipsoidal micelles were used as formulated by Pedersen.[30] In this model, the shell is described as consisting of noninteracting Gaussian polymer chains and these chains are assumed to be displaced from the core (or else the mathematical approximations will not work, as the chains overlap each other and the core); i.e., a mushroom polymer configuration is assumed. Nonpenetration of the chains into the core region is mimicked by moving the center of mass of the chains by a distance R_g away from the surface of the core, where R_g is the radius of the gyration of the chains. The form factor of the micelles $F_{mic}(q)$ comprises four terms: the self-correlation of the core, the self-correlation of the chains, the cross term between the core and chains, and the cross term between different chains. The interparticle structure factor $S(q)$ for block copolymer micelles is usually captured by the analytical solution of the Ornstein−Zernike equation with the Percus−Yevick approximation, employing hard sphere interaction.[31]

In case of polydisperse micelles, eq 2 can be written as

$$d\Sigma/d\Omega(q) = \int d\Sigma/d\Omega(q,R_c)f(R_c)dR_c + B \qquad (3)$$

The polydispersity in the micellar size ($R = R_c$) has been accounted for by a Schultz distribution as given by the equation

$$f(R_c) = [(z + 1)/R_{cm}]^{z+1}R_c^z \times \exp[-(z + 1)/R_{cm})R_c][1/(\Gamma(z + 1)] \qquad (4)$$

where R_{cm} is the mean value of the distribution and z is the width parameter. The polydispersity of this distribution is given by $\Delta R_c/R_{cm} = 1/(z + 1)^{1/2}$.

Steady State Fluorescence Studies. Steady state fluorescence spectra of pyrene were recorded using a Hitachi (Tokyo, Japan) model F-4500 spectrofluorimeter. Pyrene has been extensively used as a fluorescence probe to investigate the formation of hydrophobic microdomains by the surfactants and copolymers. The pyrene spectrum shows several vibronic peaks, and the ratio of the intensities of the third and first peaks (i.e., I_3/I_1) is a sensitive indicator of the polarity of the pyrene microenvironment.[32,33] The excitation wavelength was 335 nm, and the emission spectra were recorded from 350 to 450 nm.

Results and Discussion

Viscometry. The relative viscosities of the aqueous pluronic solutions show considerable temperature dependence owing to the changing solubility characteristics of the pluronic molecules with temperature. At temperatures 10−12 °C above the CMT,

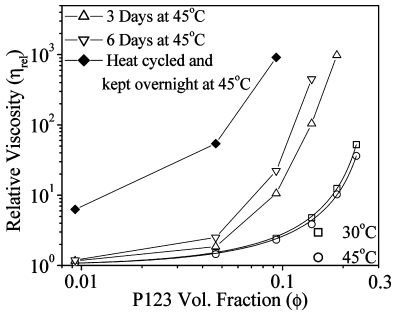

Figure 1. Relative viscosity (η_{rel}) vs P123 volume fraction plots as a function of temperature and time.

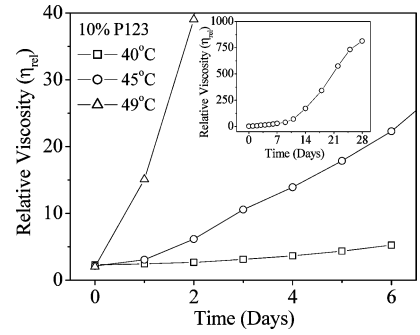

Figure 2. Relative viscosity (η_{rel}) vs time plots as a function of temperature. The inset shows the relative viscosity plot recorded at 45 °C at longer time.

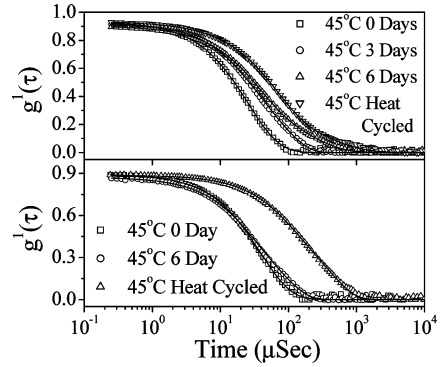

Figure 3. Correlation function diagrams of the copolymer solutions recorded at 45 °C and 130° scattering angle as a function of time and after heat cycling for (top) 10% and (bottom) 1%. The solid lines represent fits to the data.

the majority of the copolymer molecules remain in the form of micelles and the copolymer solutions can be represented as hard sphere dispersions. The relative viscosities of these solutions thus conform to the equation, $\eta_r = (1 - \phi/\phi_{max})^{-[\eta]\phi_{max}}$, where ϕ is the hard sphere volume fraction, ϕ_{max} is its limiting value at which the relative viscosity diverges, and $[\eta]$ is the intrinsic viscosity, representative of the micellar degree of hydration.[34,35] The ϕ_{max} values associated with the formation of the isotropic gel phases have been found to be close to 0.53, but due to the high degree of hydration in the micellar corona region, it is attained at the copolymer volume fraction much lower than 0.53.[36,37] Zhou et al. showed that copolymer P105 ($EO_{37}PO_{58}EO_{37}$), with a larger ethylene oxide chain and hence a much larger micellar degree of hydration than L64 ($EO_{13}PO_{30}EO_{13}$), shows divergence in relative viscosity at a lower copolymer concentration at room temperature.[38] In Figure 1, we have shown the variation of the relative viscosities of the copolymer solutions at 30 and 45 °C as a function of copolymer concentration. Since the micellar degree of hydration decreases with an increase in temperature, the relative viscosities of the copolymer concentration are found to be lower at 45 °C. An analysis of these data shows that ϕ_{max} remains constant at 0.29 but $[\eta]$ decreases with an increase in temperature from 8.45 to 7.85 cm^3/g due to a decrease in the degree of micellar hydration. The ϕ_{max} value of 0.29 agrees reasonably well with the observed gelation concentration of 28% in the case of pure P123 solutions. The $[\eta]$ values are much higher than the Einstein value of 2.5 cm^3/g for the hard sphere dispersions in solutions, which suggests that the copolymer micelles are hydrated to a significant extent and the extent of hydration decreases with an increase in temperature.

Although the copolymer solutions show smaller values of the relative viscosities at 45 °C on account of a smaller degree of micellar hydration as compared to that at 30 °C, they were found to increase over a period of several days when the copolymer solutions were maintained at 45 °C under sealed conditions. In Figure 1, we have shown the variation of the relative viscosities of the copolymer solutions with copolymer concentrations after they are kept at 45 °C for 3 and 6 days, respectively. The increment in viscosity with time is not significant at 1% copolymer solutions, but as the copolymer concentration increases, it enhances significantly and becomes a few orders of magnitude higher than the initial viscosity. Since the observed increase in viscosity with time extends up to copolymer concentrations as low as 5%, and the copolymer solutions do not phase separate all along, the presence of liquid crystalline phases may not be the reason for this unusual behavior. To understand more about this time dependent phenomenon, we have also studied the temperature dependence of viscosity and shown it in Figure 2. It is observed that the rate of viscosity enhancement increases appreciably with an increase in temperature, which can be considered as a signature of the presence of an activation barrier in the observed time dependent change in the viscosity of the copolymer solutions. In order to throw further light on the observed time dependent viscosity enhancement, we will discuss the dynamic light scattering (DLS) and small angle neutron scattering (SANS) studies on this system in the following sections.

DLS and SANS Studies. DLS studies on the 10% copolymer at 45 °C represented in Figure 3 (top) suggest that the observed increase in viscosity with time is accompanied by a shift in the correlation function vs time plots to longer time scale, which is a signature of the occurrence of a time dependent growth of the copolymer micelles. The simultaneous enhancement of micellar size and viscosity of the copolymer solutions suggests that the copolymer micelles undergo a kinetically restricted sphere-to-rod shape transition. This could arise due to the slow micellar restructuring processes required to attain the temperature dependent equilibrium structure.[19] A large aggregation number of the micelles, principally because of the highly hydrophobic nature of the copolymer molecules, and a large molecular weight of the copolymer could be the reasons behind the slow restructuring process of the P123 micelles.[19] The observed micellar growth is accompanied by a change in the nature of the plots from single exponential to biexponential, and the analysis of the data was carried out on the basis of the modified cumulants[22] method initially and a then a stretched biexponential equation after a significant micellar growth.[23−25] The results of these analyses are shown in Table 1. The stretched biexponential equation is represented as

$$g^{(1)}(t) = A_f \exp(-t/\tau_f) + A_s \exp[-(t/\tau_s)^{\beta}] \qquad (5)$$

TABLE 1: Hydrodynamic Radius (R_h), the Rod Length (L), the Stretching Exponent (β), and the Relaxation Time (τ_s) Values of the P123 Micelles As a Function of Time and Heat Treatment

sample specification	R_h (nm)	rod length (L)	τ_s (μs)	β
10% 0 day at 45 °C	8.4			
10% 3 days at 45 °C	10.9			
10% 6 days at 45 °C	12.8		159	0.78
10% (heat-cycled) at 45 °C	20.5		237	0.62
1% 0 day at 45 °C	9.5			
1% 6 days at 45 °C	13.7			
1% (heat-cycled) at 45°	39.5	266 nm (radius: 9.5 nm)		
1% 0 M NaCl at 30 °C	9.1			
1% 1 M NaCl at 30 °C	11.2			
1% 1 M NaCl (heat-cycled) at 30 °C	41.6	291 nm (radius: 9.1 nm)		
1% 1 M NaCl (heat-cycled and diluted) at 30 °C	37.4	249 nm (radius: 9.1 nm)		

where A_f and A_s are the amplitudes for the fast and slow relaxation modes corresponding to the relaxation times τ_f and τ_s, respectively.[23−25] The relaxation time for the fast mode is associated with the diffusion of the rodlike micelles, and that of the slow mode can be ascribed to coupling between concentration fluctuation and stress relaxation in entangled rodlike micelles. According to the coupling theory, the exponent β ($0 < \beta \leq 1$) is inversely proportional to the width of the distribution of the relaxation times of the slow mode, and an increase in the micellar entanglement will lead to the observation of an increase in τ_s and a decrease in β.[24] Table 1 shows that the micellar growth with time is accompanied by an increase in micellar entanglement, both of which contribute to the enhancement in the viscosity of the copolymer solutions.

Additional confirmation about the time dependent growth of the micelles could be obtained from SANS studies on the 10% copolymer solution recorded over a period of 50 h of time at 45 °C (Figure 4). An increase in the scattering cross section and a shift in the plot to lower q value are suggestive of a time dependent growth of the copolymer micelles. An analysis of these data, the results of which are shown in Table 2, indeed shows that the micelles change their shape from spherical to ellipsoidal as they grow with time. The inference about the shape change of the micelles was made on the basis of the fact that the fitting of the data recorded after 10 and 50 h of time based on the spherical shape of the micelles resulted in unacceptably high values of the normalizing constant, and micellar volume fraction values lower than even the copolymer volume fraction. The results show that quite expectedly the micellar growth with time results in an increase in the aggregation number and the aspect ratio of the copolymer micelles. The micellar volume fraction, which includes water of hydration, decreases progressively with time presumably due to the decrease in the degree of hydration of the micelles. The analysis also shows that, in spite of the observed decrease in the degree of micellar hydration with an increase in time, the hard sphere radius increases at a faster rate than the cross-sectional radius. This could be attributed to an increase in the effective volume of the intermicellar interaction arising due to an increase in the aspect ratio of the ellipsoidal shaped micelles with time.[18] These results thus suggest that the observed time dependent increase in the viscosity of the copolymer solutions is associated with a time dependent sphere-to-rod shape change of the copolymer micelles. In the following section, we will show how the kinetic barrier associated with this micellar growth can be overcome and a rapid growth of the micelles can be induced by subjecting the copolymer solutions to thermal cycling, i.e., heating them to the phase separation and subsequently cooling them back to below the cloud point.

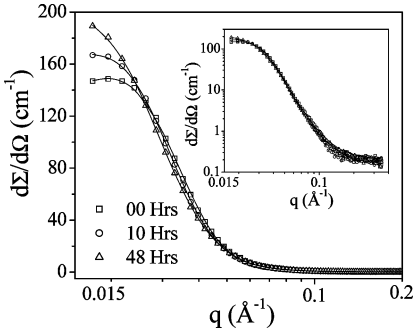

Figure 4. SANS patterns of 10% aqueous copolymer solutions with time at 45 °C. The solid lines represent fits to the data using spherical and ellipsoidal form factors. The inset shows the same plots in the logarithmic scale of the scattering intensity.

The Effect of Heat Cycling. With P123 being highly hydrophobic in nature, its aqueous solutions start becoming cloudy at temperatures as low as about 50 °C.[39,40] They, however, phase separate only at 93 °C, which has recently been reported in the literature as their cloud points.[41] In an attempt to overcome the kinetic barrier associated with the micellar growth, we have heated the copolymer solutions above 93 °C and then cooled them to 45 °C to attain clear solution. We observed that this process results in a large increase in the relative viscosity of the copolymer solutions throughout the copolymer compositions studied (Figure 1). The fact that the viscosity of the 10% copolymer solution at 45 °C approaches the viscosity achieved under heat-cycled conditions (inset of Figure 2) at a very long time suggests that the equilibrium viscosity is attained upon heat cycling as a consequence of enhancement in the micellar growth rate. Figure 3 (top) shows that the shift in the correlation function plot for the 10% heat-cycled solutions is higher than that observed in the time dependent studies up to 6 days. The difference is more conspicuous in the case of 1% solutions, which show hardly any growth with respect to time but a large growth under heat-cycled conditions (Figure 3 (bottom), Table 1). These results agree with the viscosity data shown in Figure 1, where viscosity enhancement of the 1% solutions has been shown to be significant only under heat-cycled conditions. The effect has been found to be more prominent at low copolymer concentration, which is reflected in the micellar size obtained from the analysis of these DLS data based on the modified cumulants method and stretched biexponential equation[22−25] (Table 1). We have also made an attempt to find out the cloud point of the copolymer solutions under heat-cycled conditions by keeping the heat-cycled 10% copolymer solution overnight at the different temperatures. We observed that copolymer solutions remain in the phase-separated state when they are kept at 50 °C and above, indicating that the cloud point of the solution is about 50 °C. A comparison of this cloud point value with that of 93 °C observed under normal heating conditions[41] suggests that like

TABLE 2: Core Radius (R_c), Hard Sphere Radius (R_{hs}), Aspect Ratio (ρ), Aggregation Number (N_{agg}), Volume Fraction (ϕ), and Polydispersity ($\Delta R_c/R_{cm}$) of the Micelles in 10% P123 Solutions at 45 °C as a Function of Time[a]

time (h)	R_c (nm)	ρ	N_{agg}	(R_{hs}) (nm)	(ϕ)	$\Delta R_c/R_{cm}$ (%)
00	4.75 ± 0.03		67	9.93 ± 0.04	0.183 ± 0.005	40.8 ± 0.4
10	4.61 ± 0.05	2.23 ± 0.07	137	11.24 ± 0.05	0.156 ± 0.006	19.2 ± 0.5
50	4.45 ± 0.01	3.89 ± 0.05	212	12.49 ± 0.02	0.124 ± 0.002	20.1 ± 0.2

[a] The radius of the gyration of the chains (R_g) was kept fixed at 1.2 nm as reported earlier.[36]

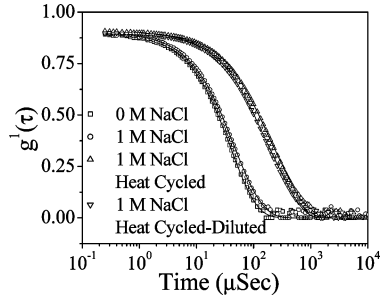

Figure 5. Correlation function vs time diagrams of 1% copolymer solutions recorded at 30 °C and 130° scattering angle. The solid lines represent fits to the data.

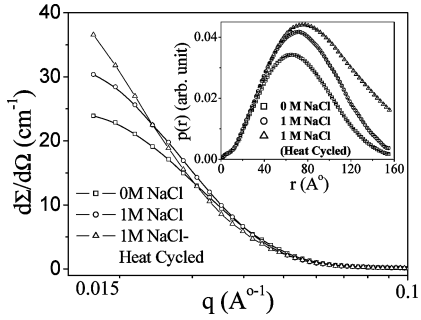

Figure 6. SANS patterns of 1% aqueous copolymer solutions recorded at 30 °C. The corresponding pair distance distribution function [$p(r)$] plots are shown in the inset.

micellar growth the phase separation process of these copolymer solutions is also kinetically restricted, and a true phase separation temperature of them can be obtained only under temperature-cycled conditions. To ensure that the heat treatments mentioned above do not lead to any significant degradation of the copolymer solutions, the viscosity, the micellar size, and the count rate (DLS studies) of the 10% copolymer solution before and after heat treatments were compared at room temperature. The practically unchanged values of these parameters suggest that copolymer solutions indeed do not undergo any significant degradation when they are subjected to different heat treatments.

The Effect of NaCl. In an effort to produce rodlike micelles at room temperature, we have also studied the effect of heat cycling on the P123 solution in the presence of NaCl. NaCl is known to increase the hydrophobic character of the copolymer molecules and reduce the CMC, CMT, gelation temperature, sphere-to-rod shape transition temperature, and cloud point of the aqueous copolymer solutions.[36,41,42] Figures 5 and 6 and Table 1 represent the DLS and SANS studies on the effect of addition of 1 M NaCl under normal and heat-cycled conditions at room temperature (30 °C). The chosen NaCl concentration is the optimum concentration for getting large micellar growth upon heat cycling with no sign of phase separation. We did not observe any significant change in the viscosity in the 1% copolymer solutions upon addition of 1 M NaCl, and Table 1 shows there is no significant growth of the micelles either. Heat cycling, however, induces a large micellar growth and an increase in the relative viscosity of the copolymer solution to

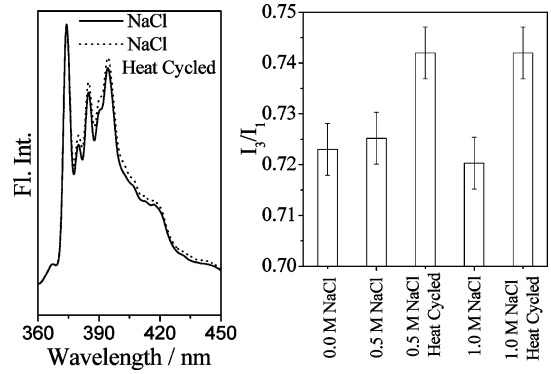

Figure 7. The fluorescence spectra of pyrene (left) and the ratio of the intensities of the third (385 nm) and first (374 nm) vibronic peaks (i.e., I_3/I_1) of pyrene (right) in 1% P123 solution under different conditions.

as high as 5.5. This suggests that the sphere-to-rod transition temperature of the micelles has been reduced to below room temperature in the presence of 1 M NaCl. The correlation function plots shown in Figure 5 highlight the micellar growth observed upon heat cycling in the form of a much larger shift in the correlation function plot to longer time scale as compared to that observed under normal conditions. The results of the analysis of the data are presented in Table 1. The SANS plots in Figure 6 show that the solutions containing 1 M NaCl show an increase in scattering intensity and a shift in the plot to lower q value upon heat cycling, which are signatures of growth of the micelles upon heat treatment. We, however, could not calculate the size of the rodlike micelles obtained under heat-cycled conditions because of our limited q region of measurement. An accurate estimation of the size of these micelles will require SANS measurement up to much lower q values that could be obtained with our instrument. Thus, to understand the micellar structure, we calculated the corresponding pair distance distribution functions [$p(r)$] using the program GENOM made by Svergun and Semenyuk.[43,44] As shown in the inset of Figure 6, the asymmetry of the $p(r)$ plot increases significantly upon heat cycling, which is a signature of enhancement in the anisotropy of the micelles leading to the formation of rodlike micelles.

Steady State Fluorescence Studies. To get a microscopic view of the consequence of heat cycling on the properties of the copolymer micelles, we have studied its effect on the I_3/I_1 peak ratio of pyrene at room temperature in the presence of NaCl. Being a nonpolar aromatic probe, pyrene preferentially resides in the less polar PPO region compared to either the hydrated PEO region (i.e., corona) or the bulk water phase. Thus, any alteration in the I_3/I_1 peak ratio is basically an indication of alteration in the hydration behavior of the micellar core. It has been observed that the ratio remains almost unaltered with the gradual addition of NaCl. However, as shown in Figure 7, there is a small increase in this ratio if the solution is heat-cycled in the presence of NaCl. This indicates that the probe microenvironment after heat cycling is less polar (more hydrophobic) compared to that in normal electrolyte solution. To note,

the smaller extent of change in the ratio is probably related to the inability of pyrene (dissolved in the PPO region) to sense the changes in the PEO region of the micelles, where electrolytes are reported to reside.[45]

The Stability of the Wormlike Micelles. In order to check whether the room temperature wormlike micelles formed in the presence of NaCl are kinetically stable or not, we have subjected the 1% heat-cycled solution to 10 times dilution and kept it at room temperature (30 °C) for 1 week. Since at this dilution the NaCl concentration present (0.1 M) is insufficient to support the wormlike structure of the micelles, the micelles should become smaller in size to get back to their spherical shape. Our DLS studies, however, show that the size of the micelles does not change significantly upon dilution, and more importantly remains practically constant with respect to time. This is reflected in the comparison of the correlation function plot of the 1% heat-cycled solutions and that of the diluted solution after 1 week, as shown in Figure 5, and the micellar size given in Table 1. The practically unchanged correlation function plot and close values of the micellar size suggest that the wormlike micelles formed upon heat cycling have significant kinetic stability, which is observed for the first time in the case of pluronics. According to recent reports, flexible wormlike micelles of bioinert copolymers are potential controlled drug release systems because of their penetrating ability into the body tissues and their minimum adhesion in flow to the cells in human blood.[46] In view of this, and the influence of the micellar disintegration on drug discharge behavior upon dilution within the human body,[47,48] the observed kinetic stability of the wormlike P123 micelles can have an important bearing on the applications of pluronics as drug delivery systems.

Conclusion

In conclusion, we have shown that the aqueous solutions of the pluronic P123 show time dependent sphere-to-rod micellar growth on approaching their cloud points. The activation energy associated with this kinetically restricted growth can be overcome and a large micellar growth can be induced if the copolymer solutions are subjected to heat cycling, i.e., heating them to the phase separation and subsequently cooling back to below their cloud points. Structure-making salts like NaCl reduce the sphere-to-rod transition temperature and help in forming wormlike micelles at room temperature upon similar heat cycling. The micelles thus formed are found to be kinetically stable with respect to dilution, which is observed for the first time in the aqueous pluronic systems.

References and Notes

(1) Chu, B. *Langmuir* **1995**, *11*, 414.
(2) Wanka, G.; Hoffmann, H.; Ulbricht, W. *Macromolecules* **1994**, *27*, 4145.
(3) Hurter, P. N.; Hatton, T. A. *Langmuir* **1992**, *8*, 1291.
(4) Schmolka, I. R. *J. Am. Oil Chem. Soc.* **1977**, *54*, 110.
(5) Pandit, N. K.; Wang, D. *Int. J. Pharm.* **1998**, *167*, 183.
(6) Zhang, K.; Khan, A. *Macromolecules* **1995**, *28*, 3807.
(7) Hvidt, S.; Jorgensen, E. B.; Brown, W.; Schillen, K. *J. Phys. Chem.* **1994**, *98*, 12320.
(8) Mortensen, K.; Brown, W.; Norden, B. *Phys. Rev. Lett.* **1992**, *68*, 2340.
(9) Malmsten, M.; Lindman, B. *Macromolecules* **1992**, *25*, 1282.
(10) Alexandridis, P.; Holzwarth, J. F.; Hatton, T. A. *Macromolecules* **1994**, *27*, 2414.
(11) Wanka, G.; Hoffmann, H.; Ulbricht, W. *Colloid Polym. Sci.* **1990**, *268*, 101.
(12) Glatter, O.; Scherf, G.; Schillen, K.; Brown, W. *Macromolecules* **1994**, *27*, 6046.
(13) Brown, W.; Schillen, K.; Almgren, M.; Hvidt, S.; Bahadur, P. *J. Phys. Chem.* **1991**, *95*, 1850.
(14) Al-saden, A. A.; Whateley, T. L.; Florence, A. T. *J. Colloid Interface. Sc.* **1982**, *90*, 303.
(15) Zhou, Z.; Chu, B. *J. Colloid Interface. Sc.* **1988**, *126*, 171.
(16) Mortensen, K.; Pedersen, J. S. *Macromolecules* **1993**, *26*, 805.
(17) Chen, W.-R.; Mallamace, F.; Glinka, C. J.; Fratini, E.; Chen, S.-H. *Phys. Rev. E* **2003**, *68*, 041402.
(18) Ganguly, R.; Choudhury, N.; Aswal, V. K.; Hassan, P. A. *J. Phys. Chem. B* **2009**, *113*, 668.
(19) Kositza, M. J.; Bohne, C.; Alexandridis, P.; Hatton, T. A.; Holzwarth, J. F. *Macromolecules* **1999**, *32*, 5539.
(20) Kositza, M. J.; Bohne, C.; Alexandridis, P.; Hatton, T. A.; Holzwarth, J. F. *Langmuir* **1999**, *15*, 322.
(21) *ASTM Standard D 445-04* and *D 446-04*, 2004, and references within.
(22) Hassan, P. A.; Kulshreshtha, S. K. *J. Colloid Interface Sci.* **2006**, *300*, 744.
(23) Moitzi, C.; Freiberger, N.; Glatter, O. *J. Phys. Chem. B* **2005**, *109*, 16161.
(24) Ngai, K. L. *Adv. Colloid Interface Sci.* **1996**, *64*, 1.
(25) Ganguly, R.; Aswal, V. K.; Hassan, P. A. *J. Colloid Interface Sci.* **2007**, *315*, 693.
(26) Koppel, D. E. *J. Chem. Phys.* **1972**, *57*, 4814.
(27) Pecora, R. *Dynamic Light Scattering: Application of Photon Correlation Spectroscopy*; Plenum Press: New York, 1985.
(28) Aswal, V. K.; Goyel, P. S. *Curr. Sci.* **2000**, *79*, 947.
(29) Pedersen, J. S.; Gerstenberg, C. *Macromolecules* **1996**, *29*, 1363.
(30) Pedersen, J. S. *J. Appl. Crystallogr.* **2000**, *33*, 637.
(31) Percus, J. K.; Yevick, G. J. *Phys. Rev.* **1958**, *1*, 110.
(32) Kalyansundaram, K. *Photochemistry in Microheterogeneous Systems*; Academic Press: Orlando, FL, 1987.
(33) Lakowicz, J. R. *Principle of fluorescence spectroscopy*, 3rd ed.; Springer: New York, 2006.
(34) De Kruif, C. G.; Van Iersel, E. M. F.; Vrij, A.; Russel, W. B. *J. Chem. Phys.* **1985**, *83*, 4717.
(35) Krieger, I. M. *Adv. Colloid Interface Sci.* **1972**, *3*, 111.
(36) Ganguly, R.; Aswal, V. K.; Hassan, P. A.; Gopalakrishnan, I. K.; Kulshreshtha, S. K. *J. Phys. Chem. B* **2006**, *110*, 9843.
(37) Ganguly, R.; Aswal, V. K. *J. Phys. Chem. B* **2008**, *112*, 726.
(38) Zhou, D.; Alexdandridis, P.; Khan, A. *J. Colloid Interface Sci.* **1996**, *183*, 339.
(39) Ganguly, R.; Aswal, V. K.; Hassan, P. A.; Gopalakrishnan, I. K.; Yakhmi, J. V. *J. Phys. Chem. B* **2005**, *109*, 5653.
(40) Chaibundit, C.; Ricardo, Nágila, M. P. S.; Ricardo, Nádja, M. P. S.; Costa Flávia de, M. L. L.; Wong, M. G. P.; Hermida-Merino, D.; Rodriguez-Perez, J.; Hamley, I. W.; Yeats, S. G.; Booth, C. *Langmuir* **2008**, *24*, 12260.
(41) Bharatya, B.; Guo, C.; Ma, J. H.; Hassan, P. A.; Bahadur, P. *Eur. Polym. J.* **2007**, *43*, 1883.
(42) Alexandridis, P.; Holzwarth, J. F. *Langmuir* **1997**, *13*, 6074.
(43) Svergun, D. I.; Semenyuk, A. V.; Feigin, L. A. *Acta Crystallogr., Sect. A* **1988**, *44*, 244.
(44) Svergun, D. I. *J. Appl. Crystallogr.* **1991**, *24*, 485.
(45) Kumbhakar, M.; Ganguly, R. *J. Phys. Chem. B* **2007**, *111*, 3935.
(46) Kim, Y.; Dalhaimer, P.; Christian, D. A.; Discher, D. E. *Nanotechnology* **2005**, *16*, S484.
(47) Pruitt, J. D.; Husseine, G.; Rapoport, N.; Pitt, W. G. *Macromolecules* **2000**, *33*, 9306.
(48) Yang, T.-F.; Chen, C.-N.; Chen, M.-C.; Lai, C.-H.; Liang, H.-F.; Sung, H.-W. *Biomaterials* **2007**, *28*, 725.

JP900535F